Environment and Ecology 37 (3A) : 854—862, July—September 2019
Website: environmentandecology.com ISSN 0970-0420

High Resolution Mapping of Solar-Induced Fluorescence using *In-Situ* Measurements and Remote Sensing Data over an Indian Mangrove Region

Kripa M. K., Ankit Gohel, Nikhil Lele, T. V. R. Murthy, Archana U. Mankad

Received 20 February 2019 ; Accepted 26 March 2019 ; Published on 17 April 2019

Abstract In this paper, the Soil Canopy Observation, Photochemistry and Energy fluxes (SCOPE) model is used for simulation of Solar–Induced Fluorescence (SIF). We have simulated SIF using *in-situ* measurements of biochemical parameters namely; chlorophyll concentration (C_{ab}), maximum carboxylation rate (V_{cmax}) for summer (May 2015), post-monsoon (December 2015) and winter (February 2016) seasons over Pichavaram mangroves, Tamilnadu. For summer season, SIF_{760} ranges from 0 to 3.2 W m^{-2} μm^{-1} sr^{-1}. In post -monsoon, SIF_{760} varies from 0 to 3.0 W m^{-2} μm^{-1} sr^{-1}. During winter season, SIF_{760} ranges from 0 to 3.6 W m^{-2} μm^{-1} sr^{-1} at 24 m resolution for Pichavaram mangroves. Dominant species map and Leaf Area Index (LAI) maps were prepared using *in-situ* measurements and Resources at-2 Linear Imaging Self-Scanning Sensor III (LISS III) data for the generation of SIF maps. Also, density wise dominant mangrove species map was generated. We have also investigated the sensitivity of SIF_{760} to biochemical parameters like V_{cmax}, C_{ab}, atmospheric temperature and vapor pressure, visible radiation and Leaf Area Index (LAI). SIF_{760} observed to be increased along with increase in LAI. However, it tends to saturate at LAI values greater than 4. The SIF_{760} varied between 0.4 and 1.3 W m^{-2} μm^{-1} sr^{-1} for all LAI values ranging from 1 to 2 and V_{cmax} of 50 µmol m^{-2} s^{-1}. It is observed that the sensitivity of SIF_{760} is large for V_{cmax} less than 200 µmol m^{-2} s^{-1} above which the SIF remains almost saturated. In future studies, it is planned to simulate for other major mangrove regions.

Keywords Mangrove, Solar-induced fluorescence, Leaf area index, Mangrove region.

Kripa M. K.*, Nikhil Lele, T. V. R. Murthy
Space Applications Center, Indian Space Research Organization, Ahmedabad, India

Kripa M. K., Archana U. Mankad
Department of Botany, Bioinformatics and Climate Change Impacts Management, University School of Sciences, Gujarat University, Ahmedabad, Gujarat, India

Ankit Gohel
Department of Physics, Government Arts and Science College, Patdi, Saurasthra University, Gujarat, India
e-mail: mrajeev777@gmail.com
*Corresponding author

Introduction

Photosynthesis is the process in which plants utilize sunlight to transform carbon dioxide and water into carbohydrate macromolecules. Fluorescence observations add a new dimension in providing a means to detect vegetation stress before chlorophyll reductions happen. Typically, less than 5% of absorbed photons are re-emitted by plants as fluorescence (Van der Tol et al. 2014). The fluorescence signal originates in the photosystems I and II. Solar-Induced Fluorescence (SIF) emitted by vegetation is seen as an expressive indicator f instantaneous plant photosynthetic activity and possibly Gross Primary Productivity (GPP) at

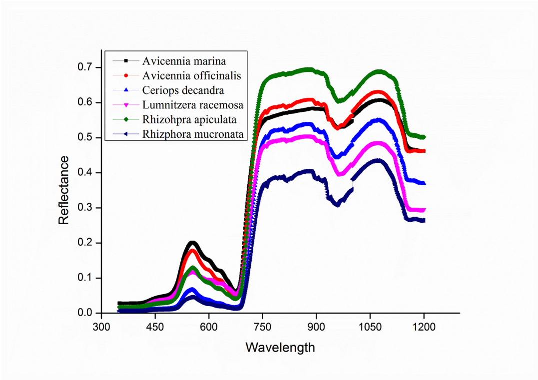

Fig. 1. Reflectance spectra of various mangrove species recorded using ASD spectroradiometer.

he ecosystem scales (Porcar - Castell et al. 2014). Since light reactions of photosynthesis, fluorescence and heat dissipation occur in competition, variation in the efficiency of one process affects the efficiencies of others. Chlorophyll fluorescence spectra have two peaks: one in red (~690 nm) and the other in far red (740 nm). Red peak is mainly contributed by Photosystem II (PSII) activity, while far-red peak is the combination of both Photosystem I (PSI) and PSII. PS II fluorescence is related to photochemical processes, which provides information on light use efficiency (Porcar-Castell et al. 2014, Meroni et al. 2009, Rossini et al. 2015, Yang et al. 2015). Regarding the water stress, a negative correlation between vapor pressure deficit and SIF is observed (Lee et al. 2013). A major advantage of the SIF signal is that it is a more physiologically related signal than reflectance and it originates exclusively from vegetation.

Several methods for detecting SIF include radiance-based and reflectance-based methods (Meroni et al. 2009). Radiance-based methods are based on the Fraunhofer Line Discriminator (FLD) principle. FLD, which was proposed by Plascyk (1975), Plascyk and Gabriel (1975), uses Sun irradiance and canopy radiance inside the Fraunhofer line and outside the line to compute the SIF. A series of methods have been developed to modify this restriction, such as 3FLD (Maier et al. 2003), corrected FLD (Moya et al. 2006), improved FLD (Alonso et al. 2008), extended FLD (Mazzoni et al. 2007) and spectral fitting methods (Meroni et al. 2010). Detection of SIF from field radiance spectra using FLD showed good correlation with Photosynthetically Active Radiation (PAR) (Liu et al. 2005). Modelled SIF using FluorMOD model and its comparison with OCO-2 observations provides SIF at 757 and 771 nm. Modelled and observed SIF had good correlation (r = 0.77) at 757 nm Pradhan and Gohel 2016). The global and regional averages as well as the zonal averages of both SCOPE based SIF and GPP are in good agreement with GOSAT based SIF. However, the peaks of the SCOPE SIF lag by 1 month than that of GOSAT based SIF in the Northern and Southern Hemispheres (Koffi et al. 2015).

The present study addresses the vegetation far-red SIF properties. The objective of the paper is to model SIF_{760} using SCOPE model from *in-situ* measurements of biochemical and biophysical parameters of major mangrove species collected during summer, post-monsoon and winter season from Pichavaram, Tamilnadu. Comparison of SCOPE SIF_{760} with LAI developed from *in-situ* measurements and Resourcesat-2 LISS III was accomplished.

Study area

Pichavaram mangrove forest (Latitude: 11.46^o N, Longitude: 79.79^o E) which was declared as a reserve forest in 1987, covers an area about 1471 ha including mangrove forests, mudflats, back waters and sand dunes. The climate is sub-humid with very warm summer and with an annual average rainfall (70 years) of 1310 mm and annual average rainy days up to 56. A total of 14 mangrove species are identified in Pichavaram mangroves, among which *Avicennia marina*, *Avicennia officinalis*, *Rhizophora mucronata*, Excoecaria agallocha, were considered for the study.

Materials and Methods

In-situ measurements of photosynthetic rate and fluorescence measurements were carried out with the instrument LI-COR LI-6400XT - Portable Photosynthesis System (LI-COR 2004). Integrated Pulse Amplitude Modulation System (PAM) and integrated Leaf Chamber Fluorometer (LCF), has the capability to simultaneously measure the chlorophyll fluorescence and photosynthesis at leaf level with the aid of its LED based fluorescence source accessory.

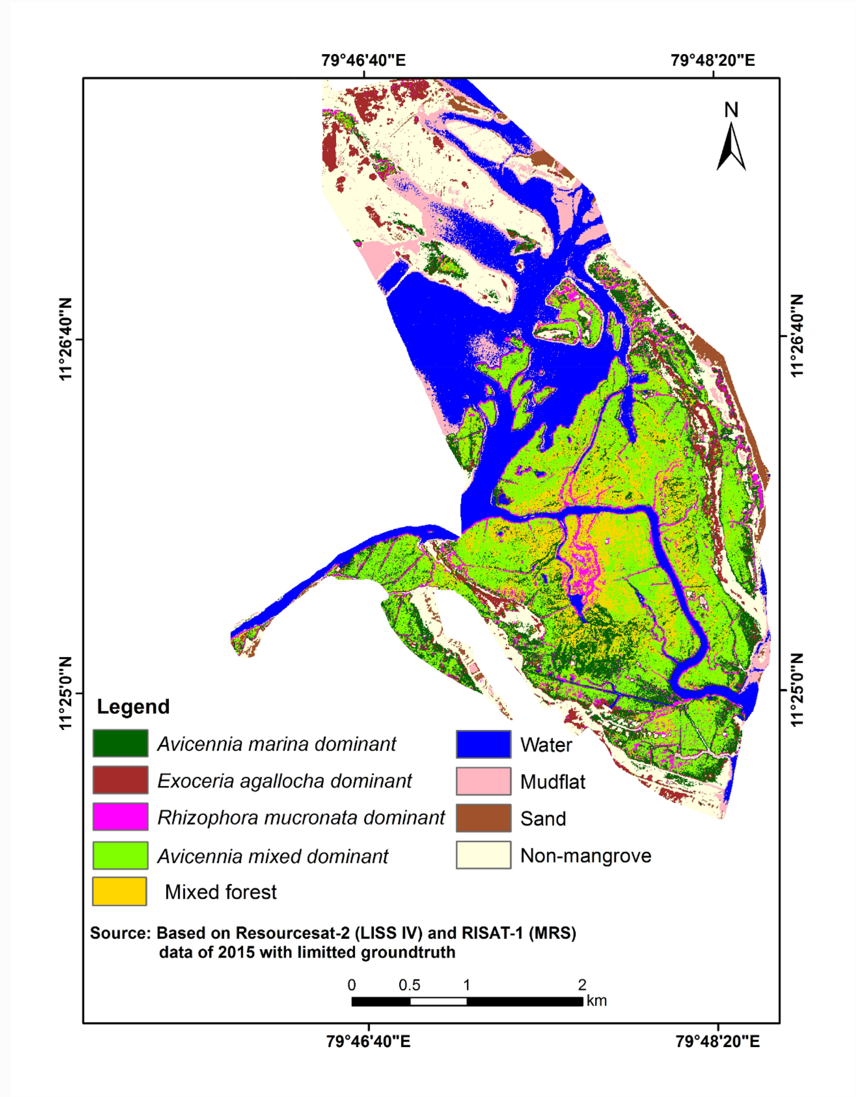

Fig. 2. Dominant vegetation map of Pichavaram mangrove using Resourcesat-2 LISS IV and RISAT-1 (MRS) data.

Non-destructive diurnal measurements of the major mangrove species at leaf level was recorded from morning 5:30 to evening 5:30 repeatedly at an interval of every 45 minutes. Two leaf samples (Sun and Shade leaves) of each species were studied to account the variability within the species. Both photosynthesis and fluorescence measurements were carried out for the same leaf throughout the day. LAI measurements were carried out with the aid of Digital Plant Canopy Imager CID Bio-science CI 110. *In-situ* measurements of chlorophyll–α, and b were carried out on the basis of Arnon's estimation method (Arnon 1949).

A total of 18 quadrats, each of 20 m × 20 m were studied for the *in-situ* measurements of LAI. From near synchronous Resourcesat-2 LISS III data, the corresponding Normalized Difference Vegetation (NDVI) values were extracted for each quadrat. A best-fit regression was derived between NDVI and LAI (r = 0.96), which was used for upscaling LAI map to 24 m resolution. Statistical analysis was done where in correlation matrices and stepwise multiple

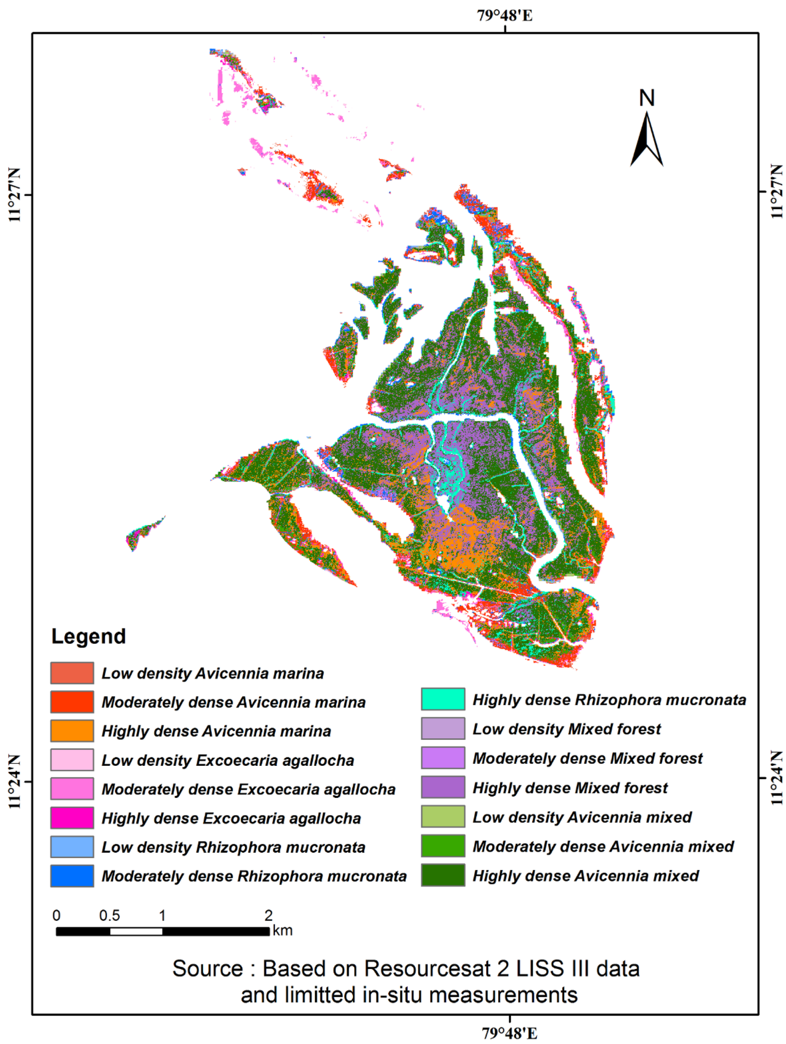

Fig. 3. Spatial layer of density-wise dominant mangroves species of Pichavaram.

regressions were used to explore the relationship between mangrove biophysical parameters with optical data. The selection of models was based on high values of correlation coefficient (R^2), high value of F-ratio and low values of standard error. The regression models, developed between LAI and radiance values of sampling locations were extended to the entire area of interest (mangrove mask). A best statistical relationship between LAI measurements was obtained from reference surface and the mean values of the corresponding optical data. Accordingly, empirical model equation (equation 1) was developed for the generation of LAI map.

$$y = 22.471x^2 - 3.0142x + 1.2227 \quad (1)$$

Spectral signatures of major mangrove species were recorded *in-situ* using spectroradiometer (ASD FieldspecPro) (Fig. 1). Seperability analysis was then carried out to verify the seperability of the species.

Table 1. Aerial extents of various mangrove species of Pichavaram.

Mangrove vegetations	Area (ha)	Area (%)
Low density *Avicennia marina*	04	0.5
Moderately dense *Avicennia marina*	58	7.4
Highly dense *Avicennia marina*	103	13.2
Low density *Excoecaria agallocha*	02	0.3
Moderately dense *Excoecaria agallocha*	27	3.4
Highly dense *Excoecaria agallocha*	08	1.0
Low density *Rhizophora mucronata*	04	0.4
Moderately dense *Rhizophora mucronata*	25	3.2
Highly dense *Rhizophora mucronata*	54	6.8
Low density *Avicennia mixed*	01	0.1
Moderately dense *Avicennia mixed*	16	2.0
Highly dense *Avicennia mixed*	160	20.3
Low density mixed forest	02	0.3
Moderately dense mixed forest	28	3.6
Highly dense mixed forest	295	37.5

Each species had a unique spectral range in each band of LISS III. Due to smaller patch size and co-existence of multiple species, only dominant vegetation denoted by a single or mix of multiple species was prepared. Both the optical and SAR data were used along with limited field observations to derive a spatial map of Dominant species of the study area based on certain decision rules (Fig. 2). Later, density - wise dominant vegetation map was generated using both field measurements and optical data at 24 m resolution (Fig. 3). The area occupied by each mangrove species as observed from satellite data could be summarized as in Table 1.

SCOPE model and input parameters

SCOPE is a vertical (1–D) integrated radiative transfer and energy balance model (Van der Tol et al. 2009). The model calculates radiation transport in a multilayer canopy as a function of the solar zenith angle and leaf orientation to simulate fluorescence in the direction of observation. The biochemical component has been updated based on Collatz et al. (1991, 1992) for C_3 and C_4 plants, respectively. It determines the illumination and net radiation of leaves with respect to their position (distance from the top of canopy in units of leaf area) and orientation (leaf inclination and azimuth angle), and the spectra of reflected and

Table 2. SCOPE parameters.

Parameters	Values	Units
Incoming short wave radiation	Depending on Months	W m^{-2}
Maximum carboxylation rate	Field data	μmol $m^{-2}s^{-1}$
Chlorophyll a+b content	Field data	μg cm^{-2}
Leaf area index LAI	0.5–4.0	/
Dry matter content	0.012	g cm
Leaf equivalent water thickness	0.009	cm
Senescent material	0.0	/
Leaf structure	1.4	/
Leaf angle distribution parameter *a*	– 0.35	/
Leaf angle distribution parameter *b*	– 0.15	/
Leaf width	0.1	m
Ball-Berry stomatal conductance	0.8	/
Dark respiration rate 25° as fraction of V_{cmax}	0.015	/
Cowan's water use efficiency	700	/
Leaf thermal reflectance	0.01	/
Leaf thermal transmittance	0.01	/

emitted radiation as observed above the canopy in the specified satellite observation geometry. SCOPE requires inputs of meteorological forcing (incoming shortwave and long wave radiation, air temperature, humidity, wind speed, and CO_2 concentration) and four categories of factors: Vegetation structure parameters, such as canopy height, leaf size, leaf angle distribution and LAI, Leaf biophysical parameters:

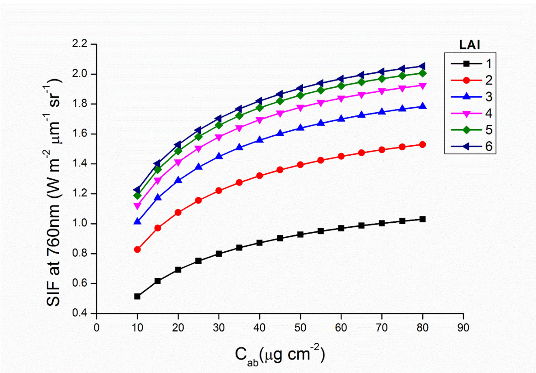

Fig. 4. Sensitivity of SIF_{760} to at C_{ab} at V_{cmax} = 75 μmol $m^{-2}s^{-1}$ and R_{in} = 500 W m^{-2}.

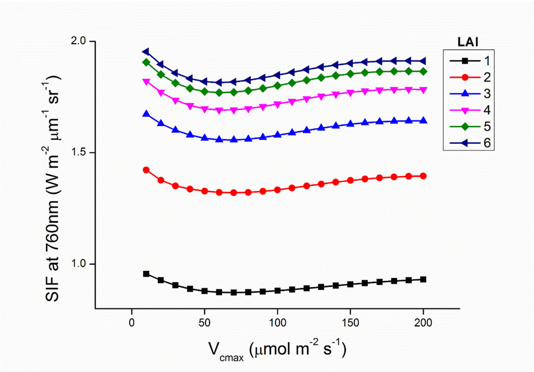

Fig.5. Sensitivity of SIF_{760} to V_{cmax} at C_{ab} = 40 μg cm^{-2} and R_{in} = 500 W m^{-2}.

Leaf chlorophyll content (C_{ab}), dry matter content (C_{dm}), leaf equivalent water thickness (C_w), senescent material (C_s) and leaf structure (N), Optical parameters: Reflectance of soil in the visible, near infrared and thermal bands and vegetation (thermal) emissivity, Plant physiological parameters: Stomatal conductance parameter (m), and maximum carboxylation capacity, V_{cmax} (Zhang et al. 2014). The required SCOPE parameters are described in Table 2. Output of the model is the spectrum of outgoing radiation in the viewing direction, turbulent heat fluxes, photosynthesis and chlorophyll fluorescence. Physical parameters were incoming short wave radiation (www.clearskycalculator.com), air temperature, air pressure, atmospheric vapor pressure, solar zenith angle and *in-situ* measurements of biochemical parameters like V_{cmax} and C_{ab}. After setting LAI, V_{cmax} and C_{ab}, SCOPE simulations was run for 1:30 pm (IST) to observe the variability of SIF in high light condition for summer, post-monsoon and winter seasons over Pichavaram mangrove. We are using LAI map and dominant mangrove species map for mapping of SIF.

Sensitivity analysis of SCOPE model

The Sensitivity of SIF to C_{ab} and V_{cmax}, the C_{ab} values varies from 10 to 80 μg cm^{-2} at every 5 μg cm^{-2} and V_{cmax} ranges from 10 to 200 μmol m^{-2} s^{-1} interval of 10 μmol m^{-2} s^{-1} respectively. From the sensitivity analysis, it is observed that SIF increases with the increase

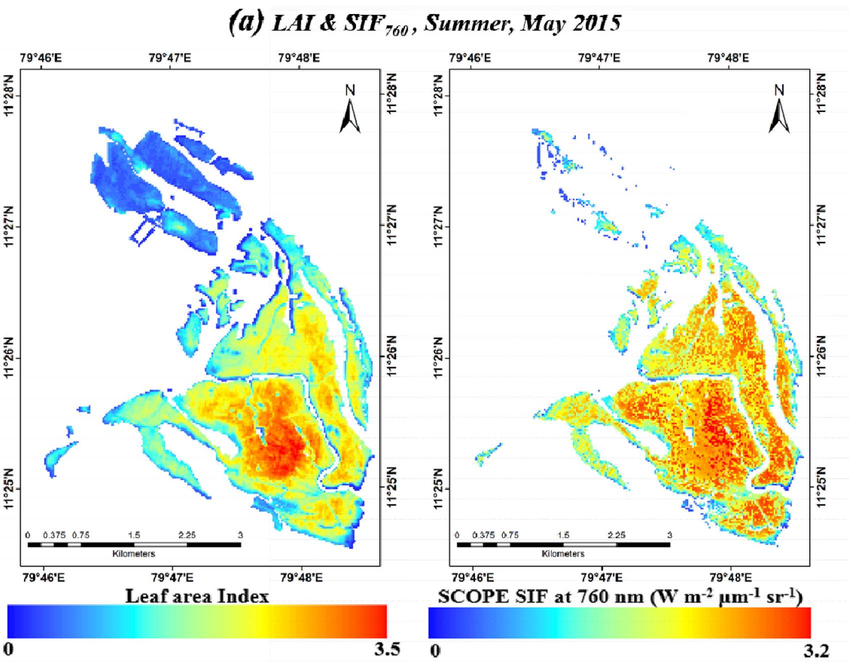

Fig. 6. (a) Modelled LAI map from *in-situ* measurements and its corresponding SCOPE SIF_{760} for (a) Summer,

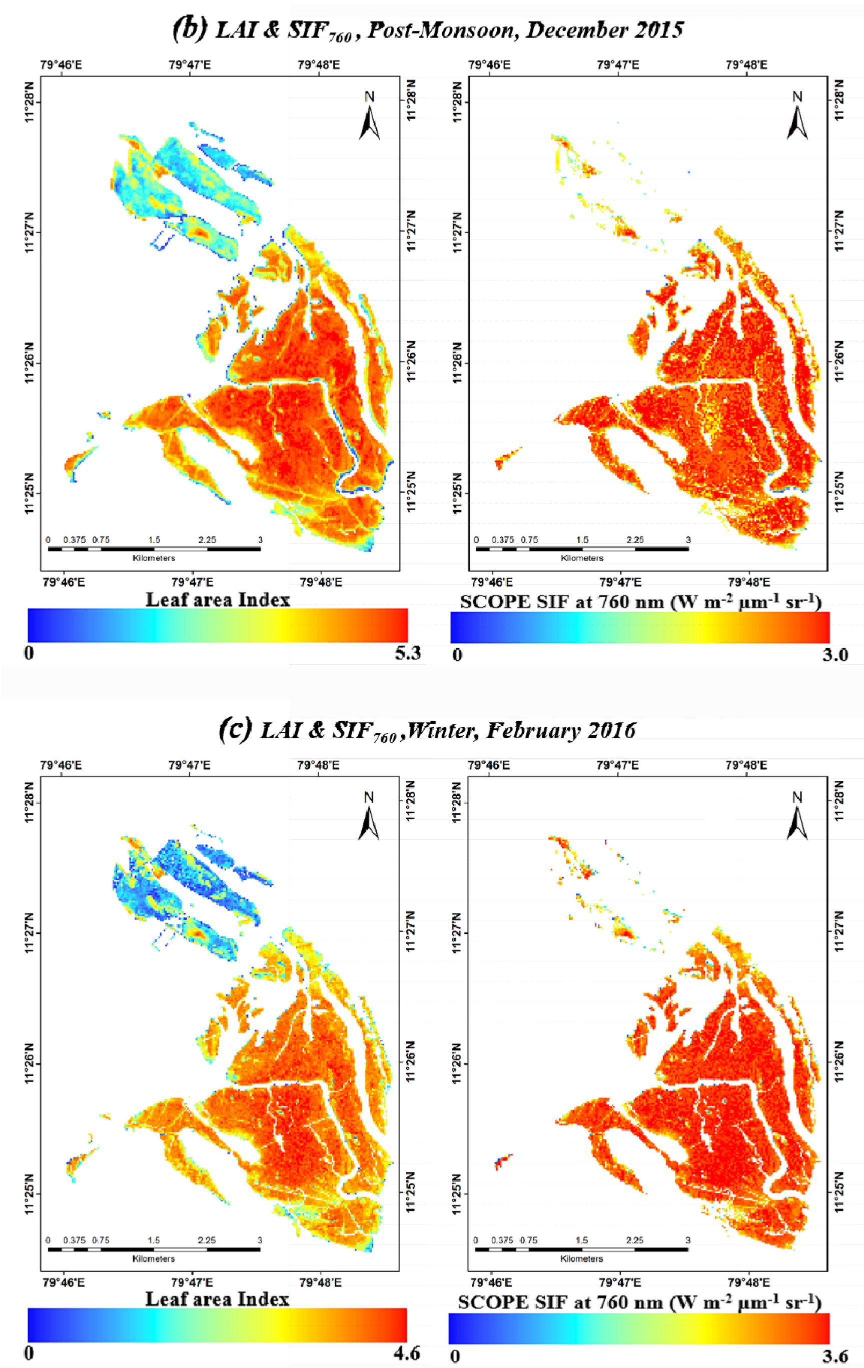

Fig. 6. Modelled LAI map from *in-situ* measurements and its corresponding SCOPE SIF_{760} for (b) Post monsoon, (c) Winter season.

of LAI. However, it tends to saturate at higher LAI values i.e. greater than 4. The maximum fluorescence observed at high LAI (>4) is attributed to the C_{ab}.

Variation of fluorescence is a function of C_{ab} and LAI. For a given LAI, SIF_{760} was highly sensitive for C_{ab} less than 20 µg cm^{-2}. For larger C_{ab} values (> 70 µg

Table 3. Modelled SIF_{760} of major mangrove species for different seasons over Pichavaram at 24 m.

Mangrove vegetation	Summer May 2015 W m^{-2} µm^{-1}sr^{-1}	Post-monsoon December 2015 W m^{-2} µm^{-1}sr^{-1}	Winter February 2016 W m^{-2} µm^{-1}sr^{-1}
Avicennia marina	1.77	2.24	2.64
Avicennia officinalis	2.38	2.76	3.32
Rhizophora mucronata	1.61	2.17	2.44
Excoecaria agallocha	0.64	0.75	0.84

cm^{-2}) SIF_{760} remained almost constant (Fig. 4). The sensitivity is large for V_{cmax} less than 100 µmol m^{-2} s^{-1} and its becomes almost constant for V_{cmax} higher than 200 µmol m^{-2} s^{-1} (Fig. 5). GPP is strongly sensitive to V_{cmax}, while SIF is more sensitive to C_{ab} and weakly sensitive to V_{cmax} under high radiation conditions and lower V_{cmax} (Koffi et al. 2015).

Results and Discussion

In our study, we simulated SIF_{760} which is the combination of both PSI and PSII. For summer season (May 2015), SIF_{760} ranged from 0.0 to 3.2 W m^{-2} µm^{-1} sr^{-1} and LAI varied from 0.0 to 3.5. In post-moonsoon (December 2015), SIF_{760} varied from 0.0 to 3.0 W m^{-2} µm^{-1} sr^{-1}with LAI ranges of 0.0 to 5.3. For winter (February 2016), SIF_{760} ranged from 0.0 to 3.6 W m^{-2} µm^{-1} sr^{-1} and LAI varied from 0.0 to 4.6 at 24 m resolution for Pichavaram mangroves (Fig. 6). SIF_{760} values for major mangrove species like *Avicennia marina*, *Avicennia officinalis*, *Rhizophora mucronata* and *Excoecaria agallocha* are listed in Table 3. From the *in-situ* measurements, it is evident that during summer season, the measured LAI and C_{ab} values were least as compared to other seasons. Post-monsoon exhibited a higher *in-situ* LAI measurement with moderate C_{ab} content. Highest C_{ab} concentration recorded was during winter season with moderate LAI.

Conclusion

Present study relates the *in-situ* biochemical parameters with modelled SIF and reveals the relationship between fluorescence and photosynthesis. SIF_{760} appears to be more sensitive to C_{ab} and faintly sensitive to V_{cmax} under high light conditions at different LAI. Highest modelled values of SIF_{760} was for the winter season owing to its higher C_{ab} values, followed by post-monsoon and summer. *Avicennia officinalis* exhibited the maximum SIF_{760} of 3.32 W m^{-2} m^{-1} sr^{-1} during winter season.

The results provide an opportunity for future work over other major mangrove regions. In the present scenario of global warming, it is advisable to plant mangroves having higher photosynthetic rate and carbon sequestration potential along the coastal regions. As the coastal areas are more prone to natural hazards like cyclones and tsunami, effective conservation and management of mangroves are recommended for the protection of shorelines.

Acknowledgement

This research work was carried out under the project Biophysical characterization and site suitability Analysis for Indian Mangroves under PRACRITI PHASE II project. Authors express sincere gratitude to Shri Tapan Misra, Director SAC, Dr. Raj Kumar, Deputy Director EPSA, Dr. Prakash Chauhan, Group Director, BPSG and Dr. B. K. Bhattacharya, Head AED for providing an opportunity and guidance to undertake this study.

References

Alonso L, Gomez-Chova L, Vila-Frances J, Amoros-Lopez J, Guanter L, Calpe J, Moreno J (2008) Improved Fraunhofer Line Discrimination Method for Vegetation Fluorescence Quantification. IEEE Geoscience and Remote Sensing Letters 5 : 620—624. doi: 10.1109/LGRS.2008.2001180.

Arnon DI (1949) Copper Enzymes in Isolated Chloroplasts Polyphenol Oxidase in Beta vulgaris. Pl Physiol 24 : 1—5. doi: 10.1104/pp.24.1.1.

Collatz GJ, Ball JT, Grivet C, Berry JA (1991) Physiological and environmental regulation of stomatal conductance, photosynthesis and transpiration: A model that includes a laminar boundary layer. Agric For Meteorol 54 : 107—136. doi: 10.1016/0168-1923 (91)90002-8.

Collatz G, Ribas-Carbo M, Berry JA (1992) Coupled photosynthesis-stomatal conductance model for leaves of C_4 plants. Aust J Pl Physiol 19 : 519—538. doi: 10.1071/PP9920519.

Koffi EN, Rayner PJ, Norton AJ, Frankenberg C, Scholze M (2015) Investigating the usefulness of satellite-derived fluorescence data in inferring gross primary productivity within the carbon cycle data assimilation system. Biogeosciences 12 : 4067—4084. doi: 10.5194/bg-12-4067-2015.

Lee JE, Frankenberg C, van der Tol C, Berry JA, Guanter L, Boyce CK, Fisher JB, Morrow E, Worden JR, Asefi S, Badgley G, Saatchi S (2013) Forest productivity and water stress in Amazonia: Observations from GOSAT chlorophyll fluorescence. Proc the Royal Soc B 280 (1761): 20130171. doi: 10.1098/rspb.2013.0171.

LI-COR (2004) Using the LI-6400 Portable Photosynthesis System Biosciences, Inc Lincoln, NE, USA. http://www.licor.-com/env/products/photosynthesis/measurements.html.

Liu L, Zhang Y, Wang J, Zhao C (2005) Detecting Solar-Induced Chlorophyll Fluorescence from field Radiance Spectra based on the Fraunhofer Line Principle IEEE Transactions Geoscience and Remote Sensing 43 (4): 827—832. doi:10.1109/TGRS.2005.843320.

Maier SW, Günther KP, Stellmes M (2003) Sun-Induced Fluorescence: A New Tool for Precision Farming. Digital Imaging and Spectral Tecniques: Applications to Precision Agriculture and Crop Physiology (digitalimaginga) 66 : 209—222.

Mazzoni M, Agati G, Del Bianco S, Cecchi G, Mazzinghi P (2007) High resolution measurements of Solar-Induced Chlorophyll Fluorescence in the Fraunhofer Ha and in the atmospheric oxygen lines. In: Proc the 3rd Int Workshop on Remote Sensing of Vegetation Fluorescences. Florence, Italy.

Meroni M, Busetto L, Colombo R, Guanter L, Moreno J, Verhoef W (2010) Performance of spectral fitting methods for vegetation fluorescence quantification. Remote Sensing Environ 114 : 363—374. doi: 10.1016/j.rse.2009.09.010.

Meroni M, Rossini M, Guanter L, Alonso L, Rascher U, Colombo R, Moreno J (2009) Remote sensing of Solar-Induced Chlorophyll Fluorescence: Review of methods and applications. Remote Sensing Environ 113 : 2037—2051. doi:10.1016/j.rse.2009.05.003.

Moya I, Daumard F, Moise N, Ounis A, Goulas Y (2006) First airborne multiwavelength passive chlorophyll fluorescence measurements over La Mancha (Spain) Fields. Proc the Second Recent Adv in Quantitative Remote Sensing, Torrent, pp 820—825.

Plascyk JA (1975) The MK II Fraunhofer line discriminator (FLD-II) for airborne and orbital remote sensing of solar-stimulated luminescence. Optic Engg 14 : 339—346. doi: 10.1117/12.7971842.

Plascyk JA, Gabriel FC (1975) The Fraunhofer line discriminator MKII—An airborne instrument for precise and standardized ecological luminescence measurements. IEEE Transactions on Instrumentation Measurement IM 24: 306—313. doi: 10.1109/TIM.1975.4314448.

Porcar-Castell A, Tyystjärvi E, Atherton J, Van der Tol C, Flexas J, Pfündel EE et al. (2014) Linking chlorophyll, a fluorescence to photosynthesis for remote sensing applications: Mechanisms and challenges. J Experim Bot 65 (15) : 4065—4095. doi: 10.1093/jxb/eru 191.

Pradhan R, Gohel A (2016) Modelling satellite-level Solar-Induced Chlorophyll Fluorescence and its comparison with OCO-2 observations. In: Proc SPIE 9880, 98800T-1, 2016. doi: 10.1117/12.2222300.

Rossini M, Nedbal L, Guanter L, Ač A, Alonso L, Burkart A, Cogliati S, Colombo R, Damm A, Drusch M, Hanus J, Janoutova R, Julitta T, Kokkalis P, Novotny J, Panigada C, Pinto F, Schickling A, Schüttemeyer D, Zemek F, Rascher U (2015) Red and far red Sun-Induced Chlorophyll Fluorescence as a measure of plant photosynthesis. Geophysic Res Letters 42 (6) : 1632—1639. doi: 10.1002/2014GL062943.

Van der Tol C, Berry JA, Campbel PKE, Rascher U (2014) Models of fluorescence and photosynthesis for interpreting measurements of Solar-Induced Chlorophyll Fluorescence. J Geophysic Res Biogeosci 119 (12) : 2312-2327. doi: 10.1002/2014JG-002713.

Van der Tol C, Verhoef W, Rosema AA (2009) Models for chlorophyll fluorescence and photosynthesis at leaf scale. Agric and For Meteorol 149 : 96—105. doi: 10.1016/j.agrformet.2008.07.007.

Yang X, Tang J, Mustard JF, Lee JE, Rossini M, Joiner J, Munger JW, Kornfeld A, Richardson AD (2015) Solar-Induced Chlorophyll Fluorescence that correlates with canopy photosynthesis on diurnal and seasonal scales in a temperature deciduous forest. Geophysic Res Letters 42 (8) : 2977—2987. doi: 10.1002/2015GL063201.

Zhang Y, Guinter L, Berry JA, Joiner J, van der Tol C, Huete A, Gitelson A, Voigt M, Köhler P (2014) Estimation of vegetation photosynthetic capacity from space-based measurements of chlorophyll fluorescence for terrestrial biosphere models. Global Change Biol 20 (12) : 3727—3742. doi:10.1111/gcb.12664.